Inorg. Chem. **2004**, *43*, 375–384

Synthesis and Characterization of New Mg_2Al-Paratungstate Layered Double Hydroxides

M. del Arco, D. Carriazo, S. Gutiérrez, C. Martín, and V. Rives*

Departamento de Química Inorgánica, Universidad de Salamanca, 37008-Salamanca, Spain

Received July 7, 2003

Layered double hydroxides (LDHs, or hydrotalcites) with Mg^{2+} and Al^{3+} cations in the mixed metal hydroxide layer and paratungstate anions in the interlayer have been prepared. Different methods have been followed: anion exchange with Mg,Al LDHs originally containing nitrate or adipate, reconstruction of the LDH structure from a mildly calcined $Mg_2Al–CO_3$ LDH, and coprecipitation. In all cases, the tungsten precursor salt was $(NH_4)_{10}H_2W_{12}O_{42}$. The prepared solids have been characterized by elemental chemical analysis, powder X-ray diffraction (PXRD), FT-IR spectroscopy, thermogravimetric (TG) and differential thermal (DTA) analyses, scanning electron microscopy (SEM) with EDX (energy-dispersive X-ray analysis), and nitrogen adsorption at –196 °C for surface area and surface texture. Most of the synthesis methods used, especially anion exchange starting from a $Mg_2Al–NO_3$ precursor at low temperature and short reaction times, lead to formation of a hydrotalcite with a gallery height of 9.8 Å; increasing the reaction temperature to 70–100 °C and maintaining short contact times leads to a solid with a gallery height of 7.8 Å. Both phases have been identified as a result of the intercalation of $W_7O_{24}^{6-}$ species in different orientations in the interlayer space. If the time of synthesis or the temperature is increased, a more stable phase, with a gallery height of 5.2 Å corresponding to a solid with intercalated $W_7O_{24}^{6-}$, is formed, probably with grafting of the interlayer anion on the brucite-like layers. All systems are microporous. Calcination at 300 °C leads to amorphous species, and crystallized $MgWO_4$ is observed at 700 °C.

Introduction

Layered double hydroxides (LDHs) constitute a family of layered compounds in some way complementary to cationic clays. They are formed by brucite-type $M(OH)_2$ layers, where a partial M^{3+} for M^{2+} substitution has taken place, and resulted in net positive charge on the metal hydroxyde layer. The positive charge of the layers is balanced by interlayer anions. The broad variety of cations, as well as anions (organic, inorganic, coordination compounds, etc.) able to be introduced in the structure, has given rise to a great interest on these materials in the past years,[1−7] especially taking into account the large number of applications they have found as adsorbents, anion exchangers, anion scavengers, catalysts, catalyst precursors, supports, etc.

It has been reported that intercalation of polyoxometalates (POMs) in the interlayer space of LDHs leads to a new class of pillared materials very effective in different adsorption and catalysis processes.[3,6−12] Incorporation of such large entities leads to formation of large cavities which are responsible for a interlayer microporosity, in addition to producing electron-acceptor and acid sites on the basic skeleton of the LDH structure. The physicochemical and catalytic properties of these systems, or of the nonstoichio-

* To whom correspondence should be addressed. E-mail: vrives@usal.es. Phone: +34 923 29 44 89. Fax: + 34 923 29 45 74.

(1) Reichle, W. T. *Solid State Ionics* **1986**, *22*, 135.
(2) Carrado, K. A.; Kostapapas, A.; Suib, S. L. *Solid State Ionics* **1988**, *26*, 77.
(3) Cavani, F.; Trifiró, F.; Vaccari, A. *Catal. Today* **1991**, *11*, 1.
(4) de Roy, A.; Forano, C.; El Malki, K.; Besse, J. P. In *Expanded Clays and other Microporous Solids*; Occelli, M. L., Robson, H. E., Eds.; Synthesis of Microporous Materials; Van Nostrand Reinhold: New York, 1992; Vol. II, p 108.
(5) Trifiró, F.; Vaccari, A. In *Comprehensive Supramolecular Chemistry*; Atwood, J. L., Davis, J. E. D., MacNicol, D. D., Vogtle, F., Lehn, J. M., Alberti, G., Bein, T., Eds.; Pergamon-Elsevier: Oxford, 1996; Vol. 7, p 251.
(6) Rives, V.; Ulibarri, M. A *Coord. Chem. Rev.* **1999**, *181*, 61.
(7) *Layered Double Hydroxides: Present and Future*; Rives, V., Ed.; Nova Sci. Pub., Inc.: New York, 2001.
(8) Drezdzon, M. A. *Inorg. Chem.* **1988**, *27*, 4628.
(9) Kwon, T.; Pinnavaia, T. J. *Chem. Mater.* **1989**, *1*, 381.
(10) Yun, S. K.; Constantino, V. R. L.; Pinnavaia, T. J. *Microporous Mater.* **1995**, *4*, 21.
(11) Kooli, F.; Jones, W. *Inorg. Chem.* **1995**, *34*, 6237.
(12) Yun, S. K.; Pinnavaia, T. J. *Inorg. Chem.* **1996**, *35*, 6853.

10.1021/ic0347790 CCC: $27.50
Published on Web 12/03/2003

metric spinels formed upon their thermal decomposition at high temperatures, may be tailored for a specific reaction, due to the large variety of combinations available from different transition metals and polyoxometalates.

Many POMs of transition metal cations (e. g., Mo, W, V, and so forth) with different structures (Keggin, Dawson, or Finke type) have been incorporated into the interlayer of LDHs.[6,8,9,13−18] The main problem found in synthesizing these materials is that the precise nature of POM is pH-dependent[19,20] and they are usually unstable under basic conditions, so a careful control of synthesis methods and conditions (e.g., pH, temperature, contact time of the LDH precursor with POM) is required.

Previous papers have described the intercalation of metatungstate anion in the interlayer of different LDHs, either from the ammonium salt or by in situ polymerization of Na_2WO_4, using LDH precursors such as $MgAl-NO_3$, meixnerite, MgAl-terephthalate, or ZnAl-terephthalate.[9,10,12,14,21,22] The basal space measured for these solids is in the 14.5−14.8 Å range, although in most of the cases a contamination with a nonlayered material, responsible for a diffraction maximum at 10−11 Å and ascribed to a magnesium polyoxometalates, has been described.

Few papers have dealt with the intercalation of paratungstate species, $H_2W_{12}O_{42}^{10-}$,[23−25] and some of them do not reach a definitive conclusion about the real existence of this species upon intercalation, or only a poorly crystallized magnesium paratungstate salt is formed. In the present paper we have tried to intercalate paratungstate anions in the interlayer of a Mg,Al hydrotalcite, following different synthesis routes. The structural, thermal, and textural properties of the prepared solids have been studied using a wide range of physicochemical techniques, including elemental analysis, powder X-ray diffraction, FT-IR spectroscopy, thermogravimetric and differential thermal analyses, scanning electron microscopy with EDX, and adsorption−desorption of N_2 at −196 °C.

Experimental Section

Sample Preparation. Different systems have been prepared following several methods and under different experimental conditions as summarized in Table 1. In all cases, the nominal Mg/Al ratio was 2.0, and ammonium paratungstate $(NH_4)_{10}H_2W_{12}O_{42}\cdot 10H_2O$ (APW, from Merck) was used. These methods include: (I) anion exchange from a Mg_2Al-NO_3 LDH using different temperatures and contact time; (II) anion exchange for a Mg_2Al-adipate LDH prepared from meixnerite; (III) reconstruction from a calcined Mg_2Al-CO_3 LDH, and (IV) coprecipitation of precursor salts.

Table 1. Synthesis Details, Chemical Composition, and X-ray Diffraction Data

sample	precursor	pH/T/t[a]	wt % W[b]	Mg/Al[c]	W/Al[c]	d(003)[d]
WN1	Mg_2Al-NO_3	6.5/50/15	37.4	2.0	1.2	14.6
WN2	Mg_2Al-NO_3	6.5/50/60	36.9	2.1	1.2	14.6; 10.4
WN5	Mg_2Al-NO_3	6.5/100/30	37.2	2.0	1.1	12.6; 10.4
WN6	Mg_2Al-NO_3	6.5/100/360	37.9	2.0	1.1	10.0
WADP	Mg_2Al-adipate	6.5/70/30	35.4	1.95	1.1	10.4
WR	Mg_2Al-CO_3	7/70/360	32.7	1.9	1.0	10.1
WCOP	coprecipitation	6.5/70/360	27.0	1.6	0.8	10−11[e]

[a] pH, temperature (°C), and contact time (min). [b] Weight percentage. [c] Molar ratio. [d] In Å. [e] Poorly crystallized.

Method (I). A Mg_2Al-NO_3 LDH precursor, with a basal spacing of 8.5 Å, was prepared following the method previously described;[26] once prepared it was maintained in suspension under nitrogen atmosphere. A portion of this suspension (108 mL, containing 4 g of Mg_2Al-NO_3) was slowly added to a solution prepared by dissolving 5.7 g APW in 200 mL of decarbonated water at 50 °C. The mixture was magnetically stirred, and pH was maintained at 6.5 (by adding 0.1 M HNO_3) under a nitrogen atmosphere for different periods of time, leading to samples WN1 (15 min), WN2 (60 min), WN3 (6 h), and WN4 (24 h). A second set of samples were obtained in a similar way, but the temperature was maintained at 100 °C for 30 min (sample WN5) or 6 h (sample WN6). In all cases, the solid was washed several times with decarbonated water by centrifugation, filtered, and dried at room temperature in a vacuum desiccator.

Method (II). The precursor was a Mg_2Al LDH containing adipate anions in the interlayer, prepared from meixnerite following the method described by Yun and Pinnavaia.[12] In some cases, swelling of the layers by incorporation of "bulk" interlayer anions, such as adipate, favors further incorporation of large anions such as POMs. A Mg_2Al-CO_3 hydrotalcite was first prepared and calcined at 500 °C for 2 h under a nitrogen flow. A portion (2 g) of the calcined solid was dispersed in 150 mL of decarbonated water in a three-neck round-bottom flask, and the suspension was stirred under a nitrogen atmosphere for 5 days in order to obtain the Mg_2Al-OH LDH. The solution of adipic acid (containing twice the amount of adipic acid required to balance the positive charge of the layers due to the Al^{3+} cations) was introduced in the flask with a syringe, and the mixture was stirred for 3 h at 50 °C. Most of the supernatant liquid was removed with a pipet, and thus, a Mg_2Al−adipate slurry was obtained. A portion of 100 mL of decarbonated, boiled water was added, and a solution of APW, at 50 °C, was added; the mixture was further stirred for 30 min at 70 °C and pH 6.5. The solid (hereafter named WADP) was washed with decarbonated water, filtered, and dried at room temperature in a vacuum desiccator.

Method (III). A Mg_2Al-CO_3 hydrotalcite was first prepared and calcined at 500 °C for 5 h under a nitrogen flow in a tubular furnace. A portion of 2 g of the calcined solid was added to a solution obtained by dissolving 6.9 g of APW in 350 mL of decarbonated water. The mixture was magnetically stirred and heated for 6 h at 70 °C under a nitrogen flow and pH = 7. The

(13) Drezdzon, M. A. In *Novel Materials in Heterogeneous Catalysis*; Terry, R., Baker, K., Burrell, L. L., Eds.; American Chemical Society: Washington, DC, 1990; p 140.
(14) Kwon, T.; Pinnavaia, T. J. *J. Mol. Catal*. **1992**, *74*, 23.
(15) López Salinas, E.; Ono, Y. *Bull. Chem. Soc. Jpn*. **1992**, *65*, 2465.
(16) Narita, E.; Kaviratna, P. D.; Pinnavaia, T. J. *J. Chem. Soc., Chem. Commun*. **1993**, 60.
(17) Ulibarri, M. A.; Labajos, F. M.; Rives, V.; Trujillano, R.; Kagunya, W.; Jones, W. *Inorg. Chem*. **1994**, *33*, 2592.
(18) Kooli, F.; Crespo, I.; Barriga, C.; Ulibarri, M. A.; Rives, V. *J. Mater. Chem*. **1996**, *6*, 1199.
(19) Pope, M. T. *Heteropoly and Isopoly Oxometalates*; Springer-Verlag: New York, 1983.
(20) MacGarvey, G. B.; Moffat, J. B. *J. Mol. Catal*. **1991**, *69*, 137.
(21) Dimotakis, E. D.; Pinnavaia, T. J. *Inorg. Chem*. **1990**, *29*, 2393.
(22) Nijs, H.; de Bock, M.; Vansant, E. F. *J. Porous Mater*. **1999**, *6*, 101.
(23) Tatsumi, T.; Yamamoto, K.; Tajima, H.; Tominaga, H. *Chem. Lett*. **1992**, 815.
(24) Gardner, E.; Pinnavaia, T. J. *Appl. Catal., A* **1998**, *167*, 65.
(25) Guo, Y.; Li, D.; Hu, Ch.; Wang, Y.; Wang, E. *Int. J. Inorg. Mater*. **2001**, *3*, 347.
(26) del Arco, M.; Gutiérrez, S.; Martín, C.; Rives, V.; Rocha, J. *J. Solid State Chem*. **2000**, *151*, 272.

solid was washed with decarbonated water, filtered, and dried at room temperature in a vacuum desiccator, leading to sample WR (Table 1).

Method (IV). A solution containing 16 g of $Mg(NO_3)_2 \cdot 6H_2O$ and 11.7 g of $Al(NO_3)_3 \cdot 9H_2O$ in 75 mL of decarbonated water was added to 150 mL of an aqueous solution containing 8.2 g of APW and 10 g of NaOH. The mixture was maintained at pH = 6−6.5 by adding 0.1 M HNO_3 and was magnetically stirred under a nitrogen atmosphere at 70 °C for 6 h. The suspension was then washed several times with decarbonated water, filtered, and dried at room temperature in a vacuum desiccator (sample WCOP, Table 1).

In all cases, the amount of APW was that required to balance the positive charge of the brucite-like layers, plus a 5% excess, as it has been reported that a large excess favors formation of impurities.[27] Some of the prepared samples were calcined at temperatures ranging from room temperature to 1000 °C in order to study their thermal stability and the structural evolution during calcination. These calcined samples will be named as "name"/*T*, where *T* stands for the calcination temperature, in °C.

Characterization. Elemental analyses for Mg, Al, and W were carried out in Servicio General de Análisis Químico Aplicado (University of Salamanca, Spain) by atomic absorption with a Mark 2 ELL-240 instrument after dissolving the samples in nitric acid. Powder X-ray diffraction (PXRD) patterns were collected on a Siemens D-500 instrument using Cu Kα radiation (λ = 1.54050 Å) and quartz as external standard. Fourier transform Infrared spectra (FT-IR) were recorded with a Perkin-Elmer FT-1730 instrument from Perkin-Elmer, using the KBr pellet technique; 100 scans were averaged to improve the signal-to-noise ratio, with a nominal resolution of 4 cm^{-1}. Differential thermal analysis (DTA) and thermogravimetric analysis (TG) were measured on DTA-7 and TG-7 instruments, respectively, from Perkin-Elmer. The analyses were carried out in flowing (30 $mL \cdot min^{-1}$) oxygen from L'Air Liquide (Spain). The nitrogen adsorption−desorption isotherms were recorded at −196 °C in a Gemini instrument, from Micromeritics, on samples previously degassed at 130 °C for 2 h by passing a nitrogen flow (from L'Air Liquide, Spain) in a Flow Prep 060 apparatus, also from Micromeritics. The surface areas were obtained by the BET method. The *t*-plot method was used to determine the total (S_t) and microporous (S_m) surface areas. SEM and energy-dispersive X-ray analysis spectroscopy (EDX) were performed using the same instrument JEOL JSM 5600 LV SEM equipped with EDXA facilities ISIS300.

Results

Elemental Analyses. Elemental analyses results are summarized in Table 1. The Mg/Al molar ratio values are very close in all cases (and also coincided with the value for the precursors used), except for sample WCOP prepared by coprecipitation, for which the value is 20% lower. This could be due to a relatively low value of pH used during coprecipitation; however, such a pH was also used for preparing samples WN1 to WN6 and sample WADP, where the Mg/Al value was 2.0 ± 0.1. So, we should conclude that the low Mg/Al value is probably due to the different synthetic route used (salt coprecipitation instead of anion exchange). Weir et al.[28] have suggested that the coprecipitation method is worse than anion exchange to prepare new LDHs with the hydrotalcite-like structure, as precipitation at pH values lower than 10 gives rise to sequential precipitation (precipitation of the trivalent cation, followed by precipitation of the divalent one) instead of simultaneous precipitation. If a too low pH value is used, unprecipitated Mg^{2+} may react with POM to give a magnesium-rich salt which crystallizes together with the layered material and blocks the pores.

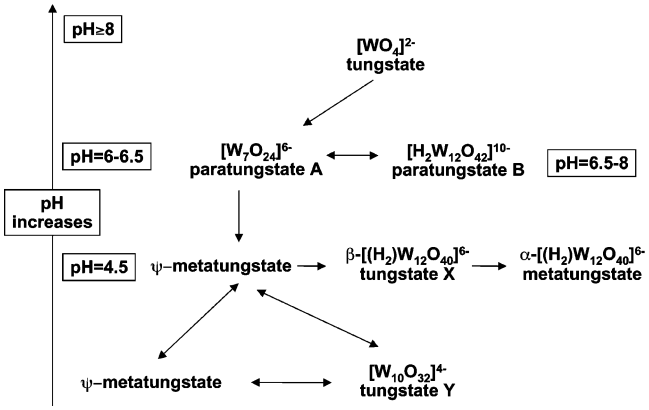

Figure 1. pH ranges corresponding to the stability of different tungsten POMs.

Small differences are also found in the tungsten content in the samples prepared by anion exchange from LDH precursors; the average value is 35.3 ± 2.6%; again, only the sample prepared by coprecipitation (sample WCOP) shows a rather lower value (27%). Among the samples prepared by anion exchange, tungsten incorporation is larger when starting from a nitrate precursor. The theoretical W/Al ratio can be calculated from the amount of aluminum in the layers and the nature of the interlayer POM balancing the positive charge of the layers, taking into account the pH at which preparation (anion exchange or coprecipitation) has been carried out (6.5−7). Figure 1 summarizes the pH ranges corresponding to the stability of the different W−POMs.[19−20] It suggests that the species most probably existing in the interlayer is $W_7O_{24}^{6-}$. Then, the theoretical W/Al ratio is 1.17. The experimental values found for the samples prepared by ion exchange are close to this value, but those for the samples prepared from adipate or carbonate LDHs are slightly lower. The value for sample WCOP is even lower (0.8 instead of 1.17).

Powder X-ray Diffraction. The PXRD patterns of representative samples are given in Figure 2; these diagrams have been recorded using the oriented aggregate method. In all cases the peaks due to diffraction by basal planes at low 2θ values ($5° \leq 2\theta \leq 10°$) indicate that the interlayer gallery has expanded; also, no peak that could be ascribed to carbonate- or nitrate-containing LDHs ($d_{(003)}$ around 7.8 or 8.5 Å, respectively) is observed, indicating that no impurity of these compounds remains in the samples. Peaks due to APW are not found either.

The diagram for sample WN1 shows diffractions at 14.6, 7.3, and 4.8 Å, which correspond to diffraction by planes (003), (006), and (009), respectively, of the layered material, confirming the hydrotalcite-like structure of this LDH.

(27) Weir, M. R.; Kydd, R. A. *Microporous Mesoporous Mater*. **1998**, *20*, 339.
(28) Weir, M. R.; Moore, J.; Kydd, R. A. *Chem. Mater*. **1997**, *9*, 1686.

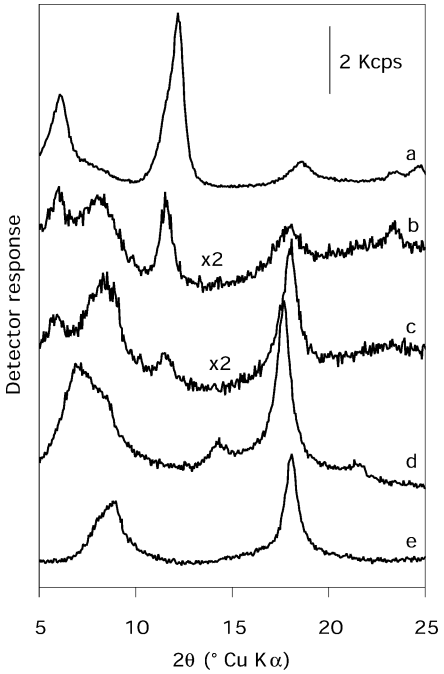

Figure 2. PXRD diagrams of samples: (a) WN1, (b) WN2, (c) WN3, (d) WN5, and (e) WN6.

Although the first order diffraction is usually the strongest one, inversion of the relative intensities of the (00*l*) planes has been reported previously.[9] Sample WN2, whose diffraction diagram is also shown in Figure 2b, was obtained following the same method as sample WN1, but the contact time between the solid and the POM solution extended for 60 min; the PXRD diagram shows weaker signals. Also, in addition to broad peaks in positions close to those reported for sample WN1, a new broad peak is recorded at 10.4 Å, and the peak at 4.8 Å in the diagram of sample WN1 has shifted up to 5 Å with parallel broadening. A peak at 3.3 Å is also now evident. These results suggest that the solid consists of two different, layered phases, with rather close *c* parameters (assuming a 3*R* stacking of the layers,[29] parameter *c* equals three times the spacing of the first harmonic, ascribed to $d_{(003)}$). With further increasing in the contact time up to 6 h (sample WN3, Figure 2c) the first set of peaks (14.6, 7.3, and 4.8 Å) has almost vanished, while for sample WN4 (the diagram has not been included in Figure 2) only the second set of maxima, with the main peak close to 10 Å, is recorded.

Alternatively, if the contact time is 30 min, but the exchange is carried out at higher temperature (100 °C, sample WN5, Figure 2d), a broad peak is recorded, where maxima at 12.6 and 10.4 Å can be identified, together with others at 6.2, 5.02 and 4.1 Å. It seems that a new phase, with harmonic maxima at 12.6, 6.2, and 4.1 Å, is being formed. An extension of the contact time to 6 h at 100 °C (sample WN6, Figure 2e) gives rise to a diagram rather similar to that for sample WN4, with a broad peak with maxima at 10 Å together with a second sharper peak at 5 Å.

The diagram for sample WADP, prepared from a Mg_2Al-adipate precursor, is essentially identical to that of sample WN3, while that for sample WR, prepared by reconstruction from a calcined Mg_2Al-CO_3 precursor, is very similar to those displayed by samples WN4 and WN6. Finally, sample WCOP, prepared by coprecipitation, shows a PXRD diagram with broad, ill defined maxima, indicating a mostly amorphous sample; for this reason, and because of the rather abnormal elemental analysis results, it has been excluded from further studies.

In order to assess if these differences in the basal spacings of the samples are due to different hydration degrees, the samples were equilibrated with water vapor for 72 h, and the PXRD diagrams were again recorded. The spacings recorded were the same as in the nonhydrated samples, suggesting they correspond to different phases, and not to a single phase under different hydration degrees.

Calcination of samples WN1, WN2, WN3, WN5, and WADP at 100 °C in oxygen leads to solids with a basal spacing close to 10 Å, as those recorded for samples WR, WN4, and WN6. Weaker and broader diffraction maxima, but in the same positions, are recorded after calcination at 300 °C (Figure 3). When the calcination temperature is further increased, amorphous phases, without well-defined diffraction maxima, are formed; the diagram for sample WN6 calcined at 500 °C is shown in Figure 3. However, calcination at 700 °C gives rise to development of weak diffraction maxima, which become sharper when calcination is carried out at 800 °C, and they have been ascribed to two different phases of $MgWO_4$: one corresponding to wolframite (file 27-789 of JCPDS files[30]), in which both tungsten and magnesium cations are octahedrally coordinated, and the other similar to an amorphous phase formed upon dehydration of $MgWO_4 \cdot xH_2O$ (file 19-776 of JCPDS files[30]),[31] in which tungsten ions are tetrahedrally coordinated and magnesium ions maintain an octahedral coordination. When the calcination temperature is increased to 1000 °C, only lines due to wolframite are recorded. The diagrams are similar to those previously recorded[32] after high-temperature calcination of solids prepared by impregnation of MgO with aqueous solutions of p-tungstate salts.

FT-IR Spectroscopy. FT-IR spectra permit detection of polytungstate existing in the sample, as well as the presence of the anions existing in the precursors used in the synthesis (i.e., carbonate, nitrate, or adipate), in case exchange had not been complete. The spectra recorded for the different samples synthesized are very similar, and representative spectra are included in Figure 4. A broad band recorded around 3460 cm^{-1} (not shown in Figure 4) is due to the stretching mode of OH groups from the brucite-like layers and of water molecules existing in the interlayer space. A medium intensity band is recorded in all cases at 1625−1630 cm^{-1}, due to the bending mode of these water

(29) Drits, V. A.; Bookin, A. S. In *Layered Double Hydroxides: Present and Future*; Rives, V., Ed.; Nova Sci. Pub. Co., Inc.: New York, 2001; Chapter 2, p 39.

(30) Joint Committee on Powder Diffraction Standards, International Centre for Diffraction Data, Pennsylvania, 1977.
(31) Gunter, J. R.; Dubler, E. *J. Solid. State. Chem*. **1986**, *65*, 118.
(32) Martín, C.; Malet, P.; Rives, V.; Solana, G. *J. Catal.* **1997**, *169*, 516.

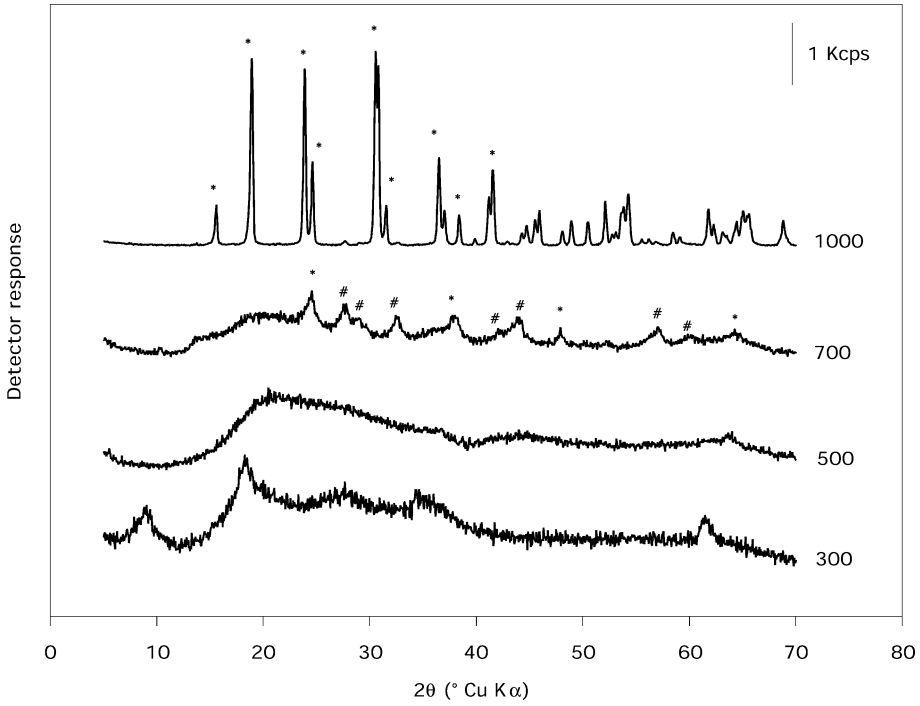

Figure 3. PXRD diagrams of sample WN6 calcined at the indicated temperatures (in °C): (*) file 27-0789; (#) file 19-0776.

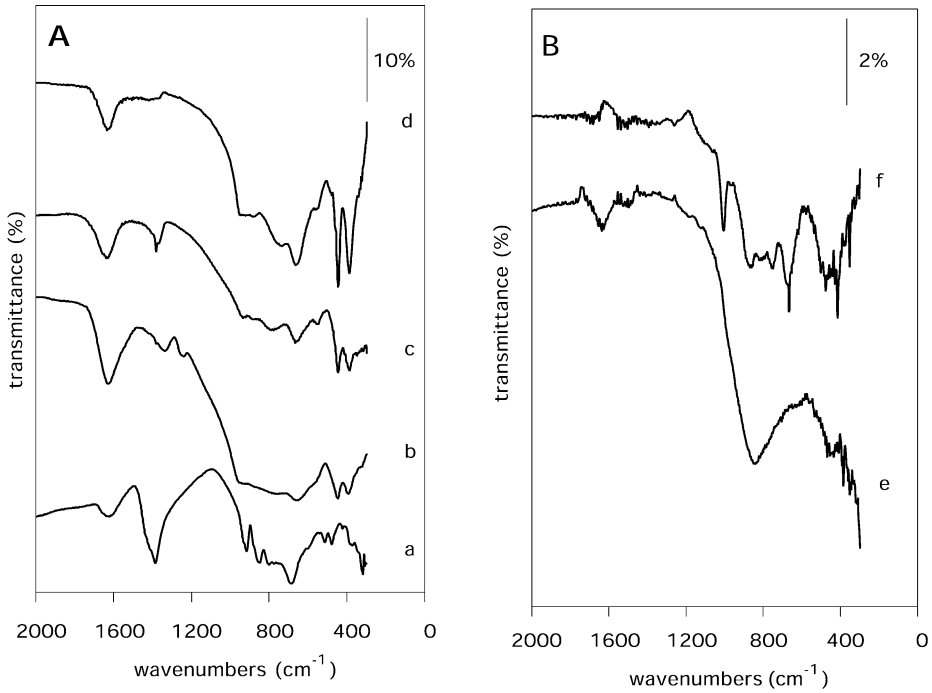

Figure 4. FT-IR spectra (KBr disks) of (A) uncalcined samples: (a) APW, (b) WADP, (c) WR, (d) WN6; (B) sample WN6 calcined at (e) 500 and (f) 700 °C.

molecules. A weak band at 1374 cm^{-1} in the spectrum of sample WR, prepared by reconstruction from a calcined Mg_2Al-CO_3 hydrotalcite, is probably due to mode ν_3 of carbonate species; as the PXRD diagram did not show any diffraction line which could be attributed to planes of this hydrotalcite, they should correspond to amorphous species or to carbonate species adsorbed on the external surface of the crystallites. However, weak bands at 1341 and 1253 cm^{-1} in the spectrum of sample WADP can be ascribed to a small amount of adipate existing in this sample, prepared from a Mg_2Al-adipate hydrotalcite precursor. The absorption band at 1384 cm^{-1}, characteristic of nitrate species, is not recorded in the spectra of the samples prepared by ion exchange from a Mg_2Al-NO_3 precursor.

The characteristic bands of polytungstate are recorded between 1000 and 500 cm^{-1}. The precise positions of these bands in some of the samples, as well as in the starting APW salt, in two calcined samples and in $W_7O_{24}^{6-}$ species, are summarized in Table 2. For the hydrotalcite-like samples, all bands are recorded in the same positions, whichever the

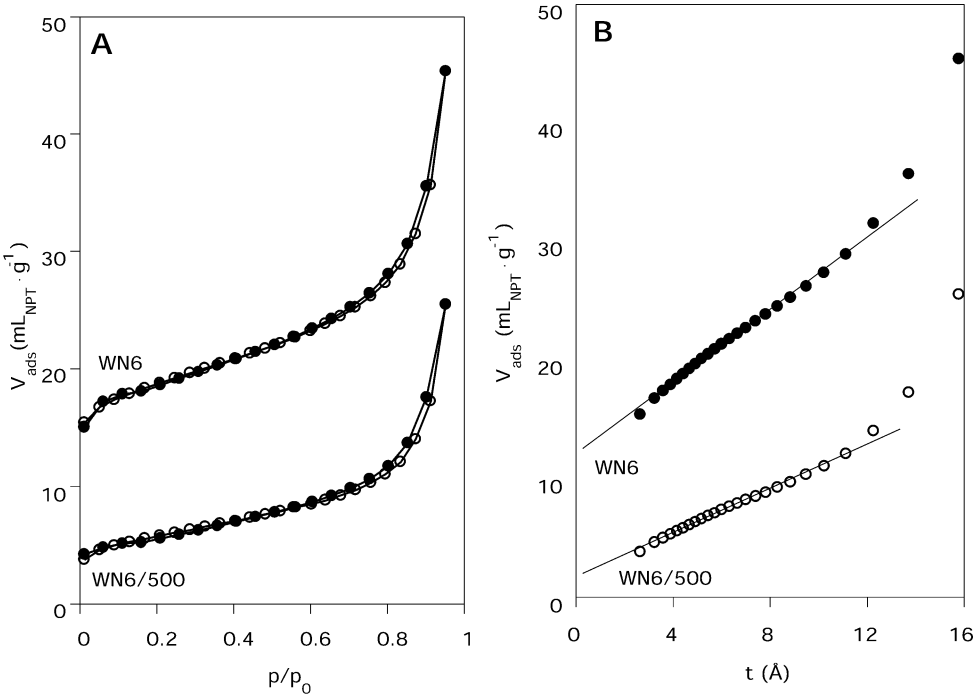

Figure 5. (A) Nitrogen adsorption−desorption isotherms (−196 °C), and (B) *t*-plots for samples WN6 and WN6/500.

Table 2. FTIR Data (cm^{-1}) of Isopolytungstate Species in the Samples Studied

sample	W=O$_d$	W−O$_b$−W	W−O$_c$−W
WN1	931	881	786, 669
WN5	950, 930	878	747, 675
WN6	950, 925	878	747, 670
WADP	958	878	797, 665
WR	931	883	786, 669
WN6/500		851	
WN6/700	1004	860, 801	751, 681
APW	934	866, 820[a]	793,[a] 702
$W_7O_{24}^{6-}$ [b]	953, 926	896, 848	668

[a] Shoulder. [b] From ref 25.

preparation method used; shifts from the positions recorded for APW are probably a consequence of the interaction of the anions with the brucite-like layers. The main bands are recorded at 958−936 cm^{-1} [terminal ν(W−O)], 881−878 cm^{-1} [corner-sharing ν_{as}(W−O−W)], and 786−746 and 669−665 cm^{-1} [edge-sharing ν_{as}(W−O−W)]. It should be recalled that the PXRD diagrams of the samples did not show any diffraction line due to starting APW, so we should conclude that the isopolytungstate species detected by FT-IR spectroscopy are intercalated between the brucite-like layers. Finally, the bands recorded below 600 cm^{-1} (close to 552, 447, and 391 cm^{-1}) are due to traslational Al/Mg−OH modes of the brucite-like layers.[33]

The FT-IR spectra of the samples calcined at 200 °C are similar to those just described for the uncalcined samples. When the calcination temperature is between 300 and 600 °C (the spectrum for the sample calcined at 500 °C is shown in Figure 4B), the bands vanish, and a broad absorption at 851 cm^{-1} dominates the spectrum. When the calcination temperature is further increased, Figure 4B, individual bands are recorded at 1004, 860, 801, 751, 681 cm^{-1}, due to stretching W−O modes of the two phases of $MgWO_4$ whose presence has been concluded from the PXRD diagram for the sample calcined at 700 °C. The intensities of these bands increase when the calcination temperature is further increased.

Surface Texture. Only samples WN6, WADP, and WR have been submitted to this study because the experimental conditions required to measure the N_2 adsorption (outgassing at 100−150 °C) are strong enough to modify the other samples. The study has been completed with sample WN6 calcined at different temperatures.

The N_2 adsorption−desorption isotherms recorded at −196 °C for sample WN6 and for this sample calcined at 500 °C (WN6/500) are included in Figure 5A. The uncalcined sample shows a typical type II isotherm shape[34] which indicates unrestricted adsorption, probably on the external surface of the crystallites. The amount of nitrogen adsorbed at low relative pressures is, however, very large, and this fact is usually associated to the presence of micropores.[35]

Layered double hydroxides with the hydrotalcite-like structure usually do not show micropores, as the interlayer space is not accessible to the N_2 molecule. However, swelling of the interlayer because of the incorporation of large anions makes this space available to adsorption as micropores,[36] but the space available for adsorption in the interlayer depends on the population of the interlayer (i.e., the number of anions

(33) Kloprogge, J. T.; Frost, R. L. In *Layered Double Hydroxides: Present and Future*; Rives, V., Ed.; Nova Sci. Pub. Co., Inc.: New York, 2001; Chapter 5, p 139.

(34) Sing, K. S. W.; Everett, D. H.; Haul, R. A. W.; Moscou, L.; Pierotti, R.; Rouquerol, J.; Sieminiewska, T. *Pure Appl. Chem.* **1985**, *57*, 603.

(35) Gregg, S. J.; Sing, K. S. W. *Adsorption Surfacre Area and Porosity*; Academic Press: London, 1982, p 208.

(36) Rives, V. In *Layered Double Hydroxides: Present and Future*; Rives, V., Ed.; Nova Sci. Pub. Co., Inc.: New York, 2001; Chapter 8, p 229.

Table 3. Textural Properties of the Samples Studied[a]

sample	S_{BET}	S_t	S_m
WR	53	26	27
WAD	72	40	33
WN6	54	25	29
WN6/200	50	n.d.	n.d.
WN6/300	20	n.d.	n.d.
WN6/500	21	17	4
WN6/700	20	17	2
WN6/900	15	n.d.	n.d.

[a] Samples had been previously degassed at 130 °C in nitrogen; values in $m^2\ g^{-1}$; n.d. = not determined. S_t = external surface area, S_m = microporous equivalent surface area, both from the *t*-plots.

balancing the positive charge of the layers due to the Mg^{2+}/Al^{3+} substitution and the formal charge of the anion), as well as of the size of the anion. The BET specific surface areas measured for our samples are summarized in Table 3. The values, for the original, uncalcined samples, range between 53 and 72 $m^2\ g^{-1}$. No significant change is observed in the S_{BET} value for sample WN6 calcined at 200 °C, but an increase in the calcination temperature gives rise to a sharp decrease in S_{BET} to 40% of the original value at 300 °C; the value remains almost constant when the calcination temperature is further increased (Table 3). Such a sharp decrease coincides with collapsing of the layered structure, as concluded from the PXRD patterns of these samples (Figure 3). Development of well crystallized $MgWO_4$ phases leads to a further decrease in S_{BET}.

Analysis of the adsorption−desorption plot following the *t*-method developed by Lippens and de Boer[37] leads to almost straight lines in the $V-t$ plots, as shown in Figure 5B for samples WN6 and WN6/500. The slight upward deviation observed at large t values is due[38] to increased uptake due to condensation in larger pores. More interestingly, extrapolated lines provide positive zero-intercepts, from which the surface area equivalent to adsorption in micropores has been calculated. As it can be seen in Table 3, such surface area represents ca. 50% of the total surface area of the solids, but it decreases to merely 10−20% for the calcined samples, confirming that collapsing of the layered structure after calcination at 500 °C and above leads to loss of microporosity.

Thermal Study. The DTA and TG patterns of the different samples are rather similar; those for sample WN6 recorded in O_2 are shown in Figure 6. Generally speaking, the pattern is similar to those previously reported for layered double hydroxides with the hydrotalcite-like structure,[39] with a broad endothermic effect in the DTA curve, centered around 180 °C, with a simultaneous weight loss amounting ca. 7−10% of the original sample weight; although analysis of evolved gases was not carried out, this weight loss is surely due to removal of interlayer water molecules, not very strongly held to the structure. The two minima recorded in the DTA curve at 361 and 408 °C are due to removal of the hydroxyl groups from the layers, as, in our case, evolution of gases by decomposition of the interlayer anion is not possible; such a process gives also rise to a weight loss of ca. 10−12% of the initial sample weight.

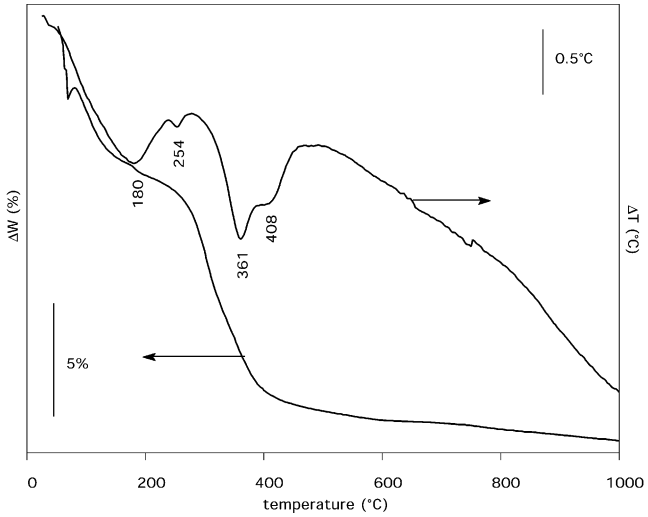

Figure 6. DTA and TG curves for sample WN6.

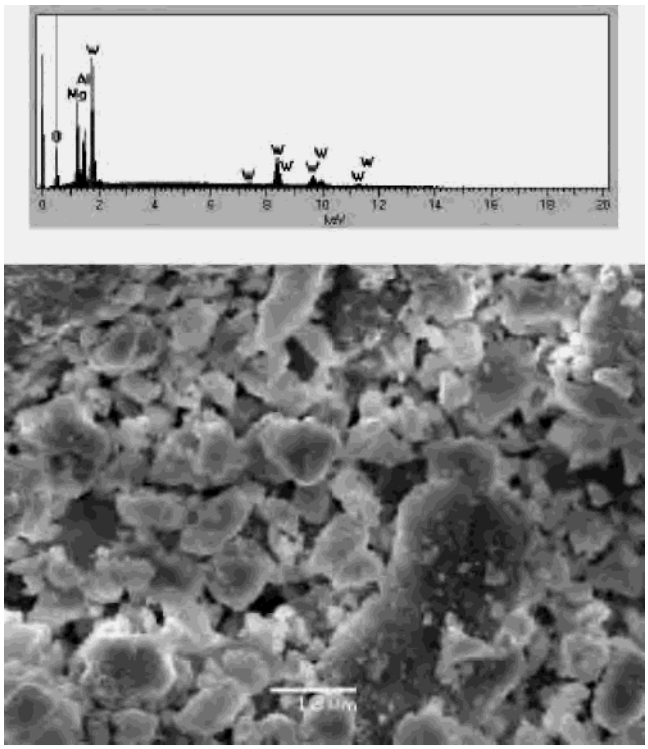

Figure 7. EDX analysis and SEM micrograph of sample WN1.

Scanning Electron Microscopy and EDX. SEM images of some of the compounds are shown in Figures 7 and 8. The images for uncalcined sample WN1 (Figure 7) and WN6 (Figure 8a) show the same crystal morphology in both cases, formed by agglomerates of rather large hexagonal platelike crystals with a diameter between 5 and 10 μm. Also shown in Figure 7 is the EDX diagram for sample WN1; similar spectra were obtained for the other uncalcined samples. The Mg/Al and Al/W atomic ratios calculated from these data

(37) Lippens, B. C.; de Boer, J. H. *J. Catal.* **1965**, *4*, 319.
(38) Lowell, S.; Shields, J. E. *Powder Surface Area and Porosity*, 2nd ed.; Chapman and Hall: London, 1984.
(39) Rives, V. In *Layered Double Hydroxides: Present and Future*; Rives, V., Ed.; Nova Sci. Pub. Co., Inc.: New York, 2001; Chapter 4, p 115.

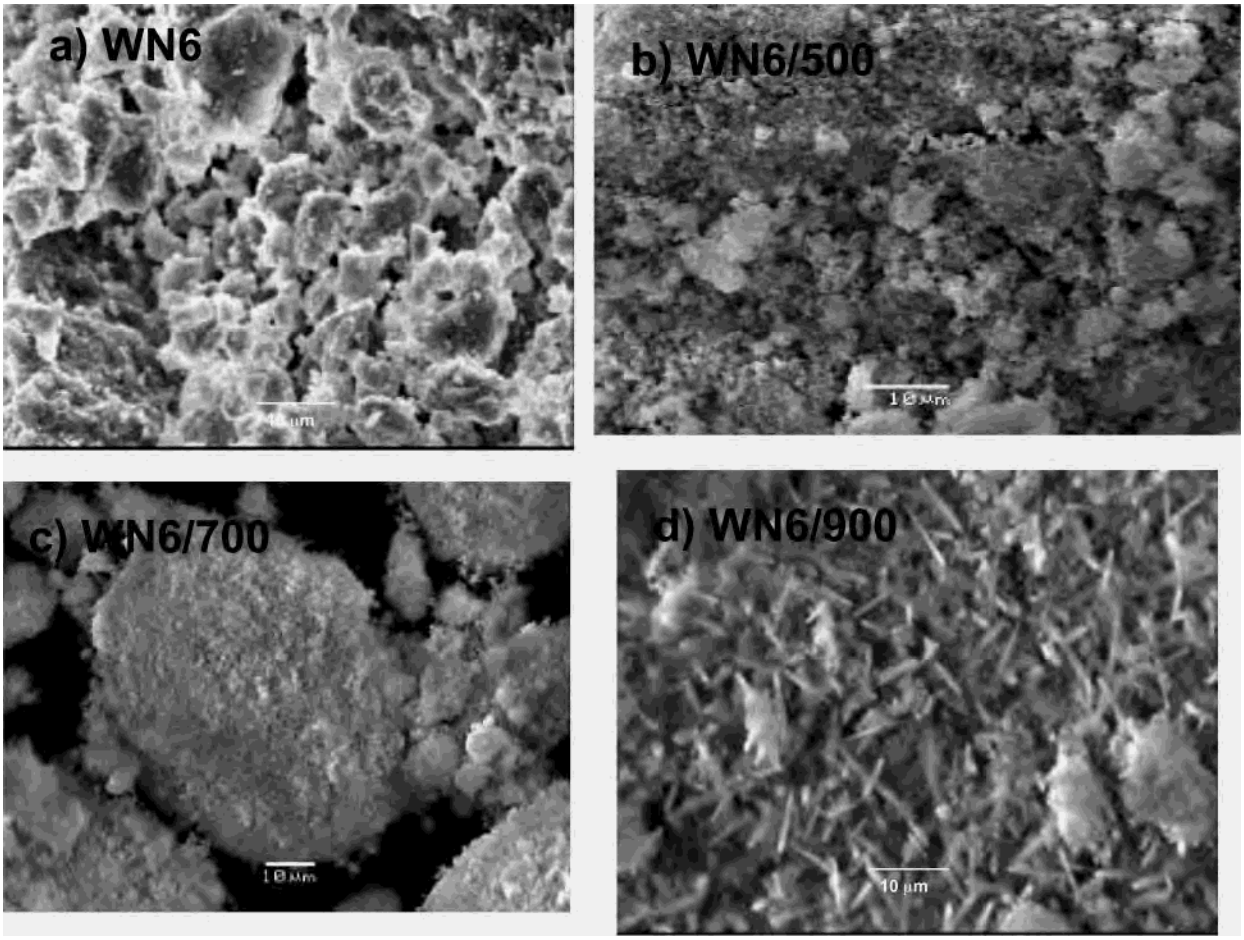

Figure 8. SEM micrographs of (a) uncalcined sample WN6, and calcined at (b) 500, (c) 700, and (d) 900 °C.

agree, within experimental error, with those calculated by elemental chemical analysis.

SEM images for calcined sample WN6 are also shown in Figure 8. Most of the crystallites show an average size close to 5 μm after calcination at 500 °C, Figure 8b. Even at 700 °C, Figure 8c, the crystallites of $MgWO_4$ are not detected at all, despite this phase being detected in the XRD diagram. However, when the sample is calcined at 900 °C, Figure 8d, needlelike crystals, characteristic of $MgWO_4$, are clearly observed.

Discussion

The $W_7O_{24}^{6-}$ anion can be oriented in two different ways in the interlayer: (a) upward and (b) parallel to the brucite layers (with the C_2 axis perpendicular to the layers), Figure 9. The height of the anion in both orientations, as determined by the Crystal Maker program[40] (once added twice the van der Waals radius of oxygen) is 9.9 and 7.5 Å, respectively. These values are very close to the gallery heights for samples WN1 and WN5 (9.8 and 7.8 Å, respectively), as calculated from the spacings experimentally measured (14.6 and 12.6 Å) and the width of the brucite layer (4.8 Å[8]). So, we can assume that in samples WN1 and WN5 the tungstate anion is oriented as shown in Figure 9a,b.

The harmonic basal reflections recorded in this study for sample WN5 are similar to those reported in previous studies on intercalation of paratungstate species[23−25] with a basal spacing (c/3) of 12 Å, with harmonic reflections at 6 and 4 Å, all three corresponding to planes (003), (006), and (009), respectively, but no previous study has reported a basal reflection of 14.6 Å, observed in our case in samples prepared at "low" temperature with short contact times, WN1. However, such spacings have been reported upon intercalation of metatungstate species.[9,10,12,14,21,22] These results might indicate that, despite us starting from paratungstate, it may have been transformed into metatungstate during the synthesis procedure. However, the pH was maintained at 6−6.5 during the synthesis of the solids, and under these experimental conditions, such a transformation can hardly occur, according to the equilibria in Figure 1. Moreover, interlayer metatungstate species are rather stable, and the characteristic PXRD lines of LDHs with intercalated metatungstate species are recorded even after heating the solid at 200 °C; however, in our case, the species formed upon intercalation are less stable and undergo transformation to another species with a basal spacing of $d_{(003)} = 10$ Å upon increasing the contact time between the precursor LDH and the paratungstate solution, and the synthesis temperature is increased or the solid obtained is heated at 100 °C. So, we should conclude that in samples WN1 and WN5 tungsten is in the form of

(40) *Crystal Maker*, version 2.1.0; http://www.crystalmaker.co.uk/crystalmaker.

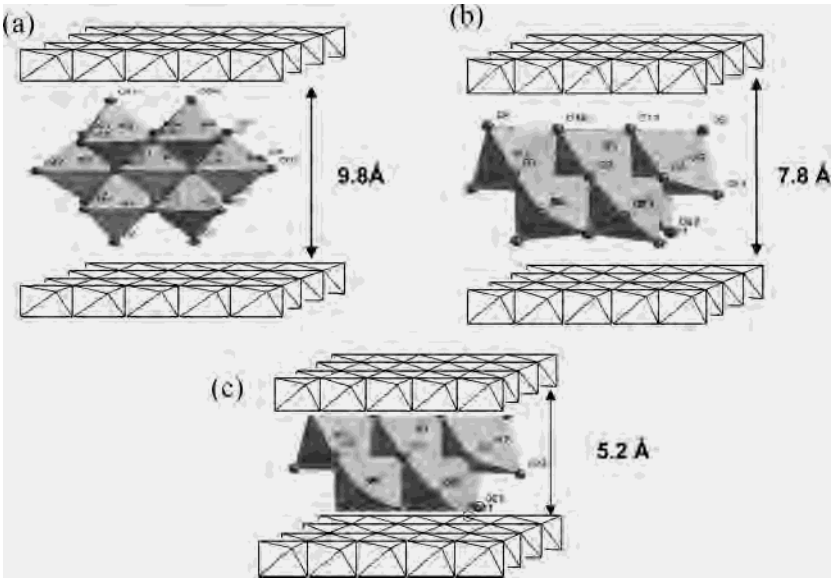

Figure 9. Models for the intercalation of paratungstate A, $W_7O_{24}^{6-}$, in samples (a) WN1, (b) WN5, and (c) WN4, WN6, and WNR. All samples calcined at 100 °C assuming grafting of the cluster to the double hydroxide layers in (c).

paratungstate A, with alternative orientations in the interlayer as shown in Figure 9a,b, depending on the temperature during synthesis.

The phase characterized by PXRD reflections at 10 and 5 Å (the only phase detected in samples WN4, WN6, and WR) has been previously reported by different authors,[8,9,11,16,21,41] in systems formed by an LDH with intercalated W or Mo polyoxometalates. Pinnavaia et al.[16] have suggested that this is a poorly ordered Mg polyoxometalate salt; however, other authors have claimed a different origin: LDHs pillared with products formed upon partial hydrolysis of the starting POM,[16,41,42] LDHs with intercalated POM grafted to the brucite-like layers by displacement of the layer OH groups by oxygen atoms of the POM, as suggested by Clearfield et al.,[41] or even a partial intercalation of POM, together with smaller anions.[42]

In our case, the results obtained seem to suggest that this phase with a basal spacing of 10 Å is an LDH with polytungstate in the interlayer. To check that it does not correspond to a magnesium p-tungstate, as claimed by some authors,[16] we have prepared this salt by direct reaction between ammonium p-tungstate and magnesium nitrate. The PXRD diagram of the solid prepared shows diffraction lines at 3.7, 2.5, and 1.6 Å which disappear upon calcination at 150 °C; these lines are not detected in the PXRD diagram of any of the LDH samples prepared in this study. The FT-IR spectrum of the salt shows bands at 859 and 564 cm^{-1}, which do not coincide with those of the LDH samples studied, and they are nonmicroporous solids. Consequently, we conclude that the solids prepared are LDHs, and not magnesium p-tungstates.

Alternatively, this phase with a basal spacing of 10 Å, detected mostly in samples WN6 and WNR, and which is more stable than the LDH prepared using short contact times between the precursor LDH and the paratungstate solution and low reaction temperatures, may be a Mg_2Al-isopolytungstate where the interlayer species could be an unidentified product formed upon hydrolysis of paratungstate A. If such a depolymerization takes place, the tungsten content in samples WN6 and WR would be lower than in the other samples. But, as shown in Table 1, they are roughly the same, especially in samples prepared by ion exchange from a nitrate LDH precursor (samples WN1 to WN6).

Consequently, we should conclude that the interlayer species is the same in all samples, $W_7O_{24}^{6-}$, and that the measured different gallery height (from 9.8 to 5.2 Å) is a result of a different interaction between the isopolytungstate anion and the brucite-like layers. Such an interaction is favored by higher temperature or longer contact times between the precursor LDH and paratungstate A. So, the phase with a basal spacing of 10 Å should correspond to structure depicted in Figure 9c, i.e., a LDH with intercalated $W_7O_{24}^{6-}$ units with the C_2 axis perpendicular to the layers, grafted to the brucite-like layers, in a similar way to the structure previously suggested by Clearfield et al.[41] for several LDH-POM systems. This would be in agreement with the PXRD diagrams recorded upon equilibrating the samples with water vapor, where no shift in the maxima was recorded, with respect to the dry samples, so confirming the strong interaction between p-tungstate and the brucite layers[43] in samples WN4, WN6, and WR.

The largest tungsten loading (37.9%) is achieved by anion exchange starting from a Mg_2Al-NO_3 LDH precursor, and complete exchange takes place. From the elemental analysis data in Table 1 and assuming the interlayer is only occupied by $W_7O_{24}^{6-}$ and water molecules, the formulas for samples WN1 and WN6 can be calculated as WN1, $[Mg_{0.67}Al_{0.33}$-

(41) Wang, J.; Tian, Y.; Wang, R. C.; Clearfield, A. *Chem. Mater*. **1992**, *4*, 1276.
(42) Weber, R. S.; Gallezot, P.; Lefebre, F.; Suib, S. L. *Microporous Mater*. **1993**, *1*, 223.
(43) Hou, X.; Bish, D. L.; Wang, S.-L.; Johnston, C.; Kirkpatrick, R. *J. Am. Mineral*. **2003**, 88.

$(OH)_2](W_7O_{24})_{0.059}\cdot xH_2O$; and WN6, $[Mg_{0.67}Al_{0.33}(OH)_2]$-$(W_7O_{24})_{0.057}\cdot xH_2O$.

Acknowledgment. We acknowledge financial support from MCyT (Grant MAT2000-1148-C02-01) and Junta de Castilla y León (Grant SA101/01). S.G. acknowledges a grant from Junta de Castilla y León. We also thank Dr. Sean Davis (School of Chemistry, University of Bristol, U.K.) for the facilities to use the electron microscope.

IC0347790